Analysis of the Schrödinger Operator in the Context of Graph Characterization

Pablo Suau[1], Edwin R. Hancock[2], and Francisco Escolano[1]

[1] Mobile Vision Research Lab, University of Alicante, Spain
{pablo,sco}@dccia.ua.es

[2] Department of Computer Science, University of York, UK
edwin.hancock@york.ac.uk

Abstract. In this paper, we apply the solution of the Schrödinger equation, i.e. the Schrödinger operator, to the graph characterization problem. The motivation behind this approach is two-fold. Firstly, the mathematically similar heat kernel has been used in the past for this same problem. And secondly, due to the quantum nature of the Schrödinger equation, our hypothesis is that it may be capable of providing richer sources of information. The two main features of the Schrödinger operator that we exploit in this paper are its non-ergodicity and the presence of quantum interferences due to the existence of complex amplitudes with both positive and negative components. Our proposed graph characterization approach is based on the Fourier analysis of the quantum equivalent of the heat flow trace, thus relating frequency to structure. Our experiments, performed both on synthetic and real-world data, demonstrate that this new method can be successfully applied to the characterization of different types of graph structures.

Keywords: graph characterization, heat flow, Schrödinger equation, quantum walks.

1 Introduction

Many physical, biological or social systems may be represented by means of a network or a graph. The analysis of graph structure and features thus becomes significant as a way of understanding the structure and dynamics of these systems. This fact hence motivated the appearance of several graph characterization techniques reported in the literature. The aim of graph characterization is to provide a way to distinguish and compare different types of graph structures without applying subgraph isomorphism, a procedure that is NP-complete. Among these graph characterization algorithms several are based on random walks [1], the Ihara zeta function [2] or the spectral radius [3]. In a recent paper, Escolano *et al.* [4] introduced an alternative technique based on the analysis of the heat flow. The heat flow is derived from the heat kernel [5], which is the solution of the heat diffusion equation, and provides a method to represent the heat transfer between nodes of a graph over time.

E. Hancock and M. Pelillo (Eds.): SIMBAD 2013, LNCS 7953, pp. 190–203, 2013.

The Schrödinger equation is mathematically similar in structure to the heat diffusion equation [6]. However, they describe rather different physical phenomena. While the heat equation describes how heat is transfered in a system, the Schrödinger equation characterizes the dynamics of a particle in a quantum system. The quantum nature of the Schrödinger equation and its complex-valued solutions give rise to many interesting non-classical effects, including quantum interferences. These interferences have proved to be useful in several applications, including the detection of symmetric motifs in graphs via continuous-time quantum walks [7] and graph embedding by means of quantum commute times [8]. Motivated by previous works on graph characterization from the solution of the heat diffusion equation, in this paper we demonstrate that the solution of the Schrödinger equation, i.e. the Schrödinger operator, may also be useful for this task. We exploit the non-ergodicity of dynamic quantum systems based on the Schrödinger equation and propose a new frequency domain characterization, based on the Fourier analysis of the quantum equivalent to the heat flow trace [4]. The resulting characterization relates frequency and graph structure. Our experiments both on synthetic and real-world datasets demonstrate that such an approach successfully distinguishes different types of network structures.

The remainder of this paper is structured as follows. In Section 2 we summarize the concept of heat flow for graph characterization. In Section 3 the Schrödinger operator is introduced. The main contributions of this paper are presented in Section 4, in which we formally analyze the Schrödinger operator and propose a new graph characterization technique based on an equivalent of the heat flow. Then, in Section 5, we show some experimental results. Finally we draw some conclusions and point out ways in which this work can be further extended.

2 Heat Flow

Let $G = (V, E)$ be an undirected graph where V is its set of nodes and $E \subseteq V \times V$ is its set of edges. The Laplacian matrix $L = D - A$ is constructed from the $|V| \times |V|$ adjacency matrix A, in which the element $A(u, v) = 1$ if $(u, v) \in E$ and 0 otherwise, where the elements of the diagonal $|V| \times |V|$ degree matrix are $D(u, u) = \sum_{v \in V} A(u, v)$. The $|V| \times |V|$ heat kernel matrix K_t is the fundamental solution of the heat equation

$$\frac{\partial K_t}{\partial t} = -LK_t, \tag{1}$$

and depends on the Laplacian matrix L and time t. It describes how information flows across the edges of a graph with time, and its solution is $K_t = e^{-Lt}$.

The heat kernel K_t is a doubly stochastic matrix. Double stochasticity implies that diffusion conserves heat. In [4], a graph is characterized from the constraints it imposes to heat diffusion due to its structure. This characterization is based on the normalized instantaneous flow $F_t(G)$ of graph G, that accounts the edge-normalized heat flowing through the graph at a given instant t, and it is defined as:

$$F_t(G) = \frac{2|E|}{n} \sum_{i=1}^{n} \sum_{j \neq i} A(i,j) \left(\sum_{k=1}^{n} \phi_k(i)\phi_k(j)e^{-\lambda_k t} \right). \tag{2}$$

A more compact definition of the edge-normalized instantaneous flow is $F_t(G) = (2|E|/n)A : K_t$, where $X : Z = trace(XZ^T)$ is the Frobenius inner product. The heat flow trace describing the graph is constructed by computing Eq. 2 on the interval $[0, t_{max}]$.

3 Heat Kernel vs. Schrödinger Operator

The Schrödinger equation describes how the complex state vector $|\psi_t\rangle \in \mathbb{C}^{|V|}$ of a continuous-time quantum walk varies with time [9]:

$$\frac{\partial |\psi_t\rangle}{\partial t} = -iL|\psi_t\rangle. \tag{3}$$

Given an initial state $|\psi_0\rangle$ the latter equation can be solved to give $|\psi_t\rangle = \Psi_t|\psi_0\rangle$, where $\Psi_t = e^{-iLt}$ is a complex $|V| \times |V|$ unitary matrix. In this paper we refer to Ψ_t as the *Schrödinger operator*. Our attention in this paper will be focused on the operator itself and not on the quantum walk process. As can be seen, Eq. 3 is similar to Eq. 1. However, the physical dynamics induced by the Schrödinger equation are totally different, due to the existence of oscillations and interferences.

In this section we address the question of whether the Schrödinger operator may be used to characterize the structure of a graph. Empirical analysis on different graph structures shows that both the heat kernel and the Schrödinger operator evolve with time in a manner which strongly depends on graph structure. [1] However, the underlying physics and the dynamics are different (see Fig. 1). In the case of heat flow heat diffuses between nodes through the edges, eventually creating transitive links (energy exchanges between nodes that are not directly connected by an edge), until reaching a stationary energy equilibrium state. The Schrödinger operator yields a faster energy distribution through the system (e.g. for a 100 nodes line graph, it takes $t = 50$ time steps for the Schrödinger operator to reach every possible position on the graph, taking more than twice this time in the case of the heat kernel [4]). Moreover, due to negative components of the complex amplitudes, interferences are created, producing energy waves. The main difference is that the Schrödinger operator never reaches an equilibrium state. In other words, it is non-ergodic. Graph connectivity imposes constraints on the distribution of energy. In the case of the heat kernel, a higher number of energy distribution constraints implies the creation of more transitive links with time [4]. This is also true in the case of the Schrödinger operator, for which lower frequency and more symmetrical energy distribution patterns are also observed.

[1] Videos showing the evolution of both heat kernel and Schrödinger operator are available at `http://www.dccia.ua.es/~pablo/downloads/schrodinger_operator.zip`

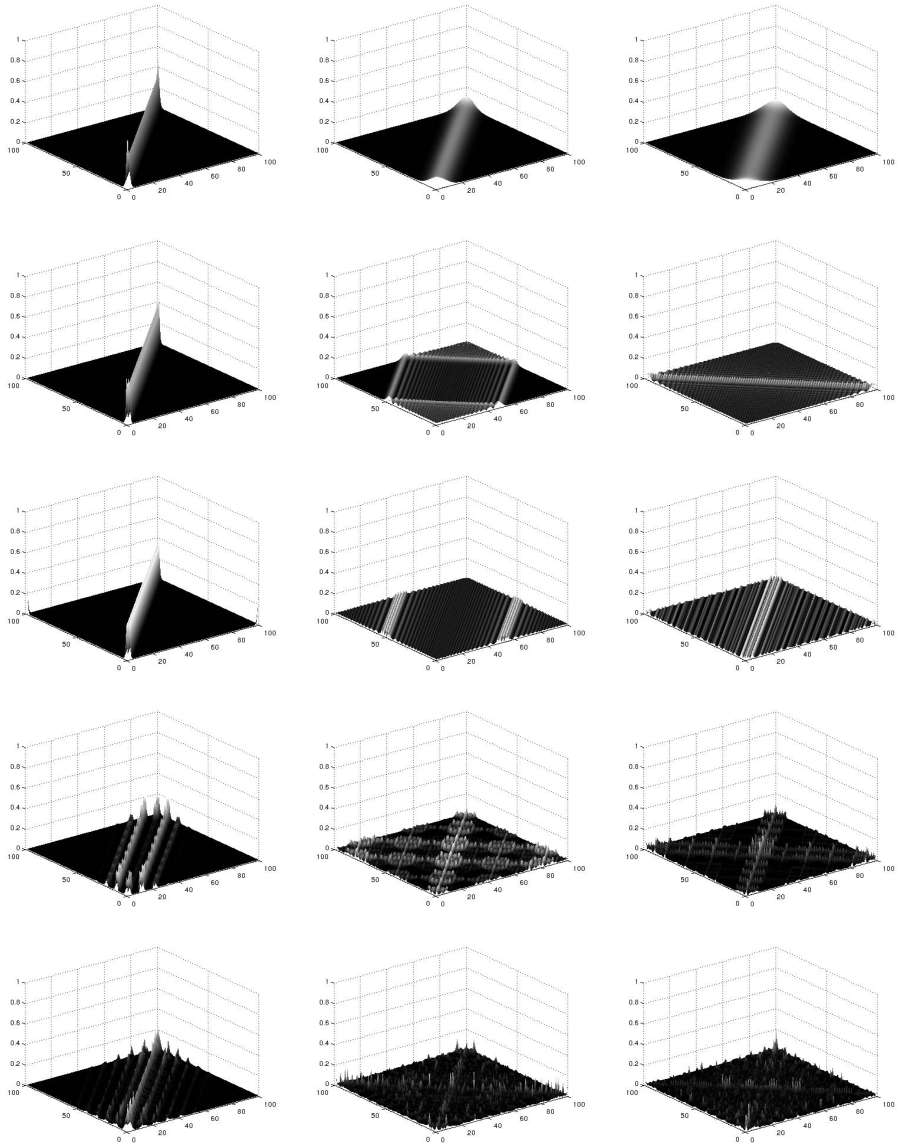

Fig. 1. Evolution with time ($t = 1, 25$ and 100). From top to bottom: heat kernel for a 100 node line graph, Schrödinger operator for a 100 node line graph, Schrödinger operator for a 100 node circle graph, Schrödinger operator for a 10×10 grid graph with 4 neighbour connectivity and Schrödinger operator for a 10×10 grid graph with 8 neighbour connectivity.

3.1 Analysis of the Schrödinger Operator

Further formal analysis of the Schrödinger operator supports the empirical evidence stated above. We first consider the Schrödinger operator when t tends to zero. Its Taylor expansion is given by:

$$\Psi t = e^{-iLt} = \cos Lt - i \sin Lt = I_{|V|} - iLt - \frac{t^2}{2!}L^2 + i\frac{t^3}{3!}L^3 + \frac{t^4}{4!}L^4 \cdots, \qquad (4)$$

where $I_{|V|}$ is the $|V| \times |V|$ identity matrix. Hence

$$\lim_{t \to 0} \Psi_t \approx I_{|V|} - iLt, \qquad (5)$$

where $\Psi_t = K_t$ when $t = 0$. At this time instant every node conserves its energy (as in the case of the Heat Kernel). The role of the identity matrix is to make the Schrödinger operator unitary. Due to the $-iLt$ term, it can be seen that energy spreads as a wave even for t values close to zero. Thus, the Schrödinger operator causes energy to distribute in a waveform from the initial time instant.

In order to explore the ergodicity of the Schrödinger operator we consider both its spectral decomposition and that of the heat kernel:

$$K_t = \sum_{p=1}^{n} e^{-t\lambda_p} \phi_p \phi_p^T \text{ and} \qquad (6)$$

$$\Psi_t = \sum_{p=1}^{n} e^{-it\lambda_p} \phi_p \phi_p^T, \qquad (7)$$

where λ_p is the p-th eigenvalue of the Laplacian L and ϕ_p its corresponding eigenvector.

The spectral decomposition of the heat kernel demonstrates that it is dominated by the lowest eigenvalues, due to the fact that $e^{-t\lambda_p}$ tends to zero as t tends to infinity. However, the limit of $e^{-it\lambda_p}$ when t tends to minus infinity is infinite. Thus, there are two important differences with the heat kernel. Firstly, the Schrödinger operator never converges (it is non-ergodic), and secondly, it is not dominated by any particular eigenvalue (i.e. there is more dependence on global graph structure as t tends to infinity).

Finally, we can compare the Euler equation based Schrödinger operator Ψ_t with the wave equation formula

$$\psi = \upsilon e^{i(kx - wt + \epsilon)}, \qquad (8)$$

where υ is the amplitude, ϵ is the initial phase, k is the wavenumber, and w is the angular frequency. The Schrödinger operator can be interpreted as a wave with $\upsilon = 1$, $k = \epsilon = 0$ and $w = L$. In fact, Eq. 7 expresses the Schrödinger operator as a linear combination of $p = 1 \ldots n$ waves with different frequencies λ_p.

3.2 The Quantum Energy Flow

As stated in Section 2 the heat flow characterizes a graph by means of a trace that accounts for the information flowing on the graph with time. Due to the similarity between the heat diffusion and the Schrödinger equations, we could define the quantum energy flow (QEF) as

$$Q_t(G) = A : \Psi_t, \tag{9}$$

and the quantum energy trace (the equivalent of heat flow) as the evolution of Q_t with time. It must be noted that the Hamiltonian of the quantum system defined by Ψ_t is given by the graph Laplacian L. The adjacency matrix A in Eq. 9 causes the QEF to only account for the energy distributing through edges. In Fig. 2 we compare the heat flow and the QEF traces for two different types of graphs. In [4], graph structure is characterized by the heat flow's phase transition point (PTP). The overall information transmitted in the system increases until reaching a PTP, and then decreases until convergence. This is illustrated inf Fig. 2 (left). A PTP based characterization can not be applied in the case of the Schrödinger operator, due to its non-ergodicity and the existence of several PTPs. However, we observe again a difference in phase transition frequency depending on the structure of the graph.

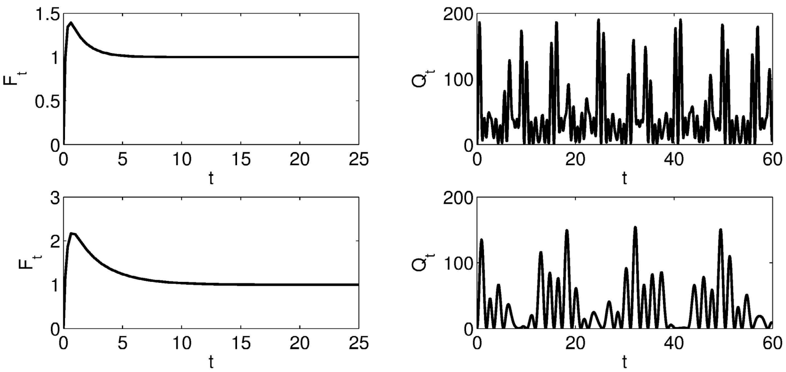

Fig. 2. Heat flow (left) and QEF (right) for two different 10 node graphs: a 2×5 grid graph with 8 neighbour connectivity (top) and a circle graph (bottom). In both cases, the x axis represents time.

3.3 Frequency Domain Analysis of the Schrödinger Operator

The results and analysis above suggest a correlation between graph structure and both the Schrödinger operator and the QEF frequency patterns. We therefore propose a graph characterization based on the QEF in the frequency domain. In order to obtain this characterization, we consider the QEF as a non-periodic signal: we select a time interval $[0, T]$ and we apply the Fast Fourier Transform to the QEF. We refer to this representation as the *frequency domain trace*. The frequency domain trace for the graphs in Fig. 2 can be seen in Fig. 3. The first conclusion from these plots is that the more complex graphs are characterized by the presence of higher frequencies.

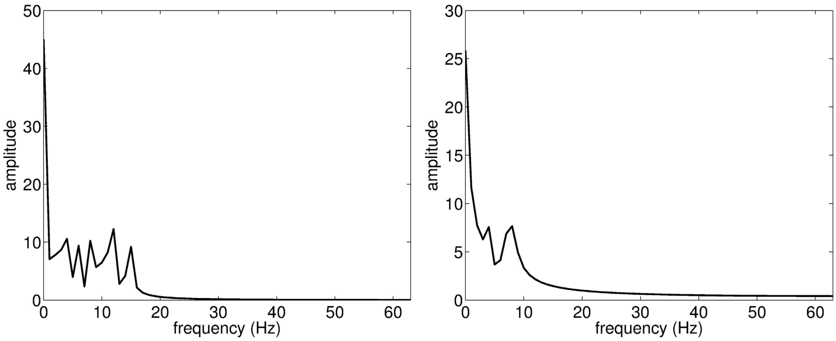

Fig. 3. Frequency domain trace obtained from the quantum energy flow of the grid graph (left) and the circle graph (right) in Fig. 2

However, this representation depends on graph size. Fig. 4 (left) shows the frequency domain trace for four differently sized line graphs. This plot demonstrates that the maximum spectral amplitude is proportional to the graph size. In order to compare arbitrarily sized graphs we apply a simple frequency domain trace normalization based on its maximum amplitude. The result of this normalization can be seen in Fig. 4 (right).

During our experiments we will represent graphs by means of a *cumulative frequency domain trace*, obtained by accumulating the normalized amplitudes

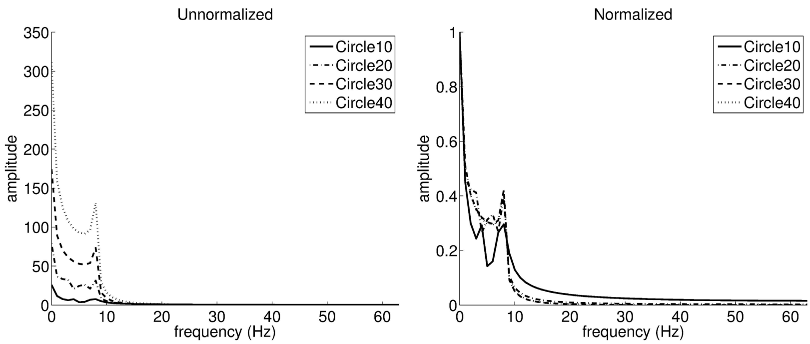

Fig. 4. Unnormalized (left) and normalized (right) frequency domain traces for four different size circle graphs (10, 20, 30 and 40 nodes)

from lower to higher frequencies of their corresponding frequency domain traces. In Fig. 5 we compare the cumulative frequency domain trace obtained from five graphs and their corresponding heat flows. In the case of the cumulative frequency domain trace, the area under the curve provides a good estimate of graph complexity. Simpler graphs yield larger areas. The PTPs of the corresponding heat flow traces also provide a good complexity estimate. In this case, the PTP for simple graphs is reached later in time. However, in this particular example, the heat flow trace estimates the complexity of the line graph to be lower than that of the circle graph. That is not the case of the cumulative frequency domain trace, for which the complexity of the line graph is higher.

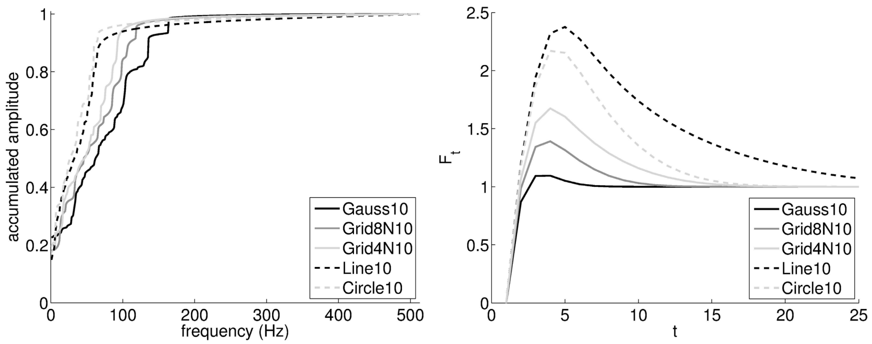

Fig. 5. Cumulative frequency domain traces (left) and heat flow (right) for five simple 10 node graphs: a random graph (Gauss10), a 8-connected 2x5 grid (Grid8N10), a 4-connected 2x5 grid (Grid4N10), a line graph (Line10) and a circular graph (Circle10)

4 Experimental Results

4.1 Noise Sensitivity

The aim of this first experiment is to show the sensitivity of frequency domain traces to graph noise. We first constructed a base 400 nodes random graph by means of the Erdös-Rényi model [10]. We then compared the frequency domain trace of the base graph to those obtained after applying random edit operations on it. In this experiment we only applied edge removal operations, and thus, in each iteration, we remove a random edge from the base graph and we compute the Euclidean distance between the unnormalized traces. The results are shown in Fig. 6. Four experiments were performed, using four different time intervals $[0..T]$ to construct the frequency domain traces.

From Fig. 6, it is clear that the final trace is not strongly affected by small disturbances. For larger time intervals there appears to be a significant sensitivity to noise. However, difference between traces is still low. The remainder of the experiments in this paper are conducted after setting $T = 1024$.

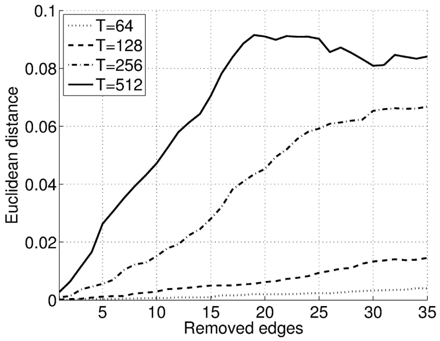

Fig. 6. Results of the noise sensitivity experiment. Number of edit operations (edge removals) versus distance between edited graph's frequency domain trace and base graph's one, for four different T values.

4.2 Characterization of Synthetic Data

In order to test the discriminative power of our characterization we constructed a dataset of synthetic graphs. The dataset consists of three groups of 32 graphs, each group characterized by a different graph structure. All of the graphs in the dataset have 90 nodes. The graphs in the first group are random graphs constructed using the Erdös-Rényi [10] model, in which each pair of nodes is linked by an edge with probability given by p. In our experiments we set $p = 0.1$. The graphs in the second group belong to the category of scale free graphs (i.e. graphs for which its degree distribution follows a power law), and were constructed using the Barabási and Albert's model [11]. In this model we have set $m_0 = 5$ for the initial size of the graphs and $m = 2$ for the number of links to add during each iteration, following the addition of a node. Finally, the graphs in the third group correspond to small world graphs (i.e. graphs in which most nodes are not neighbours of each other, but in which average path length between a graph pair of nodes is small). These small world graphs are generated by means of the Watts and Strogatz algorithm [12]. In this case we set the mean degree value to $K = 10$ and the rewiring probability to $p = 0.2$.

A cumulative frequency domain trace was computed for all graphs in the set, and the results are shown in Fig. 7. The first conclusion of our experiment is that these traces clearly discriminate between different graph structures. This conclusion is supported by a Multidimensional Scaling analysis (MDS) of the traces (also shown in Fig. 7). The aim of MDS is to apply dimensionality reduction on data while preserving relative distances between patterns. If we project the traces onto a 2D space, the graphs in the three groups are clearly split into three different clusters with high intra-cluster homogeneity and high-inter cluster separability.

In Fig. 7 we explore the relationship between frequency and structure. The frequency spectrum of random graphs is characterized by higher amplitudes at high frequencies. In the case of small world graphs, the predominant frequencies

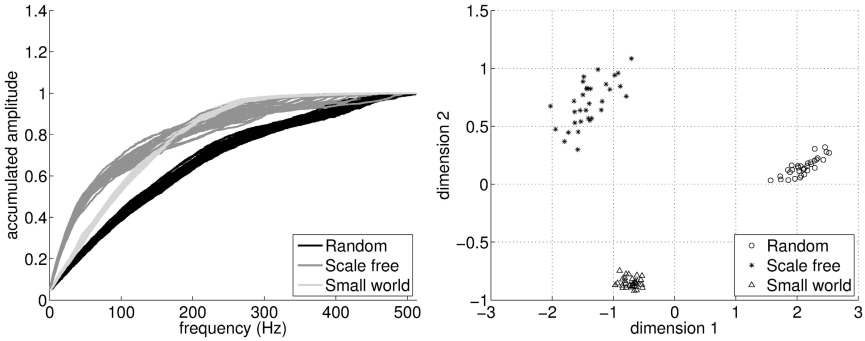

Fig. 7. Characterization of synthetic graphs. Left: cumulative frequency domain traces. Right: MDS results.

are in the middle part of the spectrum. Scale free graphs are characterized by higher amplitudes at lower frequencies. These results suggest that the structure of random graphs is more complex in the sense that it imposes more constraints to the distribution of energy on the graph. As a consequence, energy waves exhibit higher frequency as they propagate. Scale free and small world graphs impose less restrictions on the distribution of energy through the graph, and are associated with lower frequency patterns.

4.3 Characterization of Real-World Data

Our aim in this experiment was to evaluate the validity of our method when applied to real-world data. The 24 graphs studied in this experiment are part of a dataset that has been previously utilized for complex network characterization [14] or network robustness assessment [15]. Our subset of graphs is divided into two categories: a) 9 networks having a homogeneous degree distribution and b) 15 networks having a power law degree distribution. The first category consists of the following graphs: Benguela, Reef Small, Coachella Valley, Shelf, Skipwith, St. Marks Seagrass and Stony food webs and two Macaque visual cortex networks. The second category contains a more heterogeneous set of graphs: four software networks (Abi, Digital, VTK and XMMS), a network of sexual partners in Colorado Springs, a network of injectable drugs users, the airport transportation network in the US in 1997, the Scotch Broom food web, two transcription interaction networks concerning E. Coli and yeast and five different protein interaction networks. In Fig. 8 we show the cumulative frequency domain traces for all the aforementioned graphs. It must be noted that all of them vary widely in size and edge density.

The results of this experiment demonstrate that the relationship between frequency and structure is also held in the context of real-world data. Networks having a homogeneous degree distribution are not characterized by any predominant frequency. Therefore, this type of network produces an almost diagonal

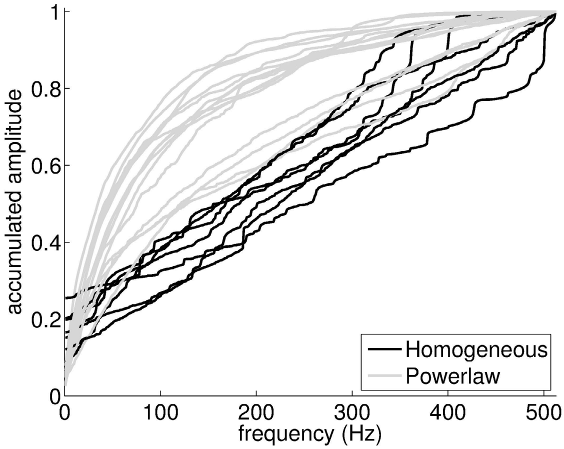

Fig. 8. Characterization of real-world networks

cumulative frequency domain trace. Networks following a power law degree distribution are mainly characterized by lower and medium frequencies. Power law degree distribution arise as a feature of scale free networks, in which there exist nodes with a degree that greatly exceeds the average in the network. This kind of structure is commonly associated with the existence of *hub* nodes that increase the overall robustness of the network, thus improving network connectedness. This observation again supports that the correlation between the lack of constraints to energy propagation on the graph and the predominance of lower frequencies in its characteristic trace.

4.4 Network Dynamics Analysis

In this last experiment we apply our characterization method to the analysis of dynamic network structures, in order to test if such characterization can give an insight into the existence of structural changes with time. We computed the traces for several graphs generated according to the activity-based preferential attachment (APA) model [16]. This model has proved to be the best approximation of the evolution of several real-world cortical networks. The APA model is a generalization of the Barabási and Albert's model, in which new connections are established proportionally to a dynamical process on the entire network, rather than according to a local structural property. Nodes with higher activity have a higher probability of establishing new connections. In the APA model, the activity of a node i is computed from the stationary distribution π of frequency of visits to nodes of a random walk, where $\pi_i = \lim_{t \to \infty} v_i/t$ and v_i the number of times the random walker visits the node i after t time steps.

The plot in Fig. 9 shows the evolution of the APA cumulative frequency domain trace over time for one of the realizations of the model. The plots obtained from other realizations were very similar. Network evolution starts at $t = 0$ with a fully connected network having 5 nodes. At each time step a new node is added, following the APA model. The process is repeated until $t = 1000$. It must be noted that the graphs constructed using the this model are directed. They were converted to undirected ones by simply transforming each directed arc into an undirected edge before computing the graph characteristic trace.

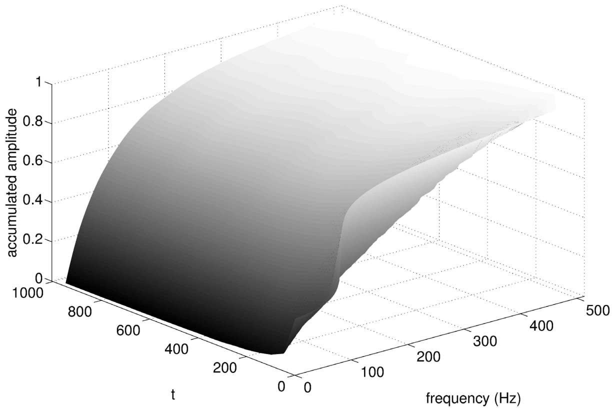

Fig. 9. Cumulative frequency domain trace over time for one dynamic graph

The results show that the structure of a graph modeled by means of activity-based preferential attachment is not subject to significant changes after an early stage in the evolutionary process. This was the expected outcome of the experiment since the APA model is intended to conserve the overall structural properties of the network through time. Moreover, this experiment shows that network growth does not have an impact on its cumulative frequency domain trace as long as global structure is conserved due to the frequency domain normalization process, making the cumulative frequency domain trace capable of comparing the structure of networks having a different amount of nodes.

5 Conclusions and Future Work

Heat flow, based on the heat kernel, has been successfully used to characterize graph structure. The aim of the present paper was to answer the question of whether the Schrödinger operator (the solution to the Schrödinger equation) can be used also to characterize graph structure. After analyzing energy distribution through the graph based on the Schrödinger operator, we introduced a new characterization method based on the analysis in the frequency domain of the quantum equivalent of the heat flow trace that relates frequency to graph structure. Experiments performed both on synthetic and real-world datasets show that the *cumulative frequency domain trace* is a useful tool for graph analysis, that is not sensitive to small changes in graph structure.

However, based on these promising preliminary results, further in depth analysis is required. Firstly, and similarly to heat flow, the cumulative frequency domain trace does not provide us with a quantitative measure to directly compare graph structures. A first step in this direction could be to apply this trace as part of the thermodynamic depth complexity measurement framework, in order to obtain a numerical representation of graph structure [4][13]. Secondly, during our analysis of the Schrödinger operator we detected the presence of symmetric energy distribution patterns on the graph. We could analyze how this symmetry depends on graph structure and whether the results of this analysis are related to previous work on symmetry detection based on quantum walks [7]. Finally, an additional future work idea comes from the results of the experiment on the dynamic dataset. This experiment proved that it would be of great interest to extend our algorithm to the directed graphs domain.

References

1. Aziz, F., Wilson, R.C., Hancock, E.R.: Graph Characterization via Backtrackless Paths. In: Pelillo, M., Hancock, E.R. (eds.) SIMBAD 2011. LNCS, vol. 7005, pp. 149–162. Springer, Heidelberg (2011)
2. Peng, R., Wilson, R.C., Hancock, E.R.: Graph Characterization vi Ihara Coefficients. IEEE Transactions on Neural Networks 22(2), 233–245 (2011)
3. Das, K.C.: Extremal Graph Characterization from the Bounds of the Spectral Radius of Weighted Graphs. Applied Mathematics and Computation 217(18), 7420–7426 (2011)
4. Escolano, F., Hancock, E.R., Lozano, M.A.: Heat Diffusion: Thermodynamic Depth Complexity of Networks. Physical Review E 85(3), 036206(15) (2012)
5. Xiao, B., Hancock, E.R., Wilson, R.C.: Graph Characteristics from the Heat Kernel Trace. Pattern Reognition 42(11), 2589–2606 (2009)
6. Aubry, M., Schlickewei, U., Cremers, D.: The Wave Kernel Signature: A Quantum Mechanical Approach To Shape Analysis. In: IEEE International Conference on Computer Vision (ICCV), Workshop on Dynamic Shape Capture and Analysis (4DMOD) (2011)
7. Rossi, L., Torsello, A., Hancock, E.R.: Approximate Axial Symmetries from Continuous Time Quantum Walks. In: Gimel'farb, G., Hancock, E., Imiya, A., Kuijper, A., Kudo, M., Omachi, S., Windeatt, T., Yamada, K. (eds.) SSPR&SPR 2012. LNCS, vol. 7626, pp. 144–152. Springer, Heidelberg (2012)
8. Emms, D., Wilson, R.C., Hancock, E.R.: Graph Embedding Using Quantum Commute Times. In: Escolano, F., Vento, M. (eds.) GbRPR. LNCS, vol. 4538, pp. 371–382. Springer, Heidelberg (2007)
9. Farhi, E., Gutmann, S.: Quantum Computation and Decision Trees. Physical Review A 58, 915–928 (1998)
10. Erdös, P., Rényi, A.: On Random Graphs. I. Publicationes Mathematicae 6, 290–297 (1959)
11. Barabási, A.L., Albert, R.: Emergence of Scaling in Random Networks. Science 286(5439), 509–512 (1999)

12. Watts, D.J., Strogatz, S.H.: Collective Dynamics of 'Small-World' Networks. Nature 393(6684), 440–442 (1998)
13. Han, L., Escolano, F., Hancock, E., Wilson, R.: Grapph Characterizations From Von Neumann Entropy. Pattern Recognition Letters 33(15), 1958–1967 (2012)
14. Estrada, E.: Quantifying Network Heterogeneity. Physical Review E 82(6), 066102 (2010)
15. Estrada, E.: Network Robustness to Targeted Attacks. The Interplay of Expansibility and Degree Distribution. The European Physical Journal B - Condensed Matter and Complex Systems 52(4), 563–574 (2006)
16. Antiqueira, L., Rodrigues, F.A., Costa, L.F.: Modeling Connectivity in terms of Network Activity. J. Stat. Mech., L09005 (2009)